

# Ultrathin Films of Perylenedianhydride and Perylenebis(dicarboximide) Dyes on (001) Alkali Halide Surfaces

D. Schlettwein,<sup>\*,†</sup> A. Back,<sup>‡</sup> B. Schilling,<sup>‡</sup> T. Fritz,<sup>§</sup> and N. R. Armstrong<sup>\*,‡</sup>

*Institut für Angewandte und Physikalische Chemie, Fachbereich Chemie, Universität Bremen, D-28334 Bremen, Germany; Department of Chemistry, University of Arizona, Tucson, Arizona 85721; and Institut für Angewandte Photophysik, Technische Universität Dresden, D-01062 Dresden, Germany*

*Received August 26, 1997. Revised Manuscript Received November 25, 1997*

Ultrathin films of two perylene dyes, 3,4,9,10-perylenetetracarboxylicdianhydride (PTCDA) and *N,N*-di-*n*-butylperylene-3,4,9,10-bis(dicarboximide) (C4-PTCDI), have been grown on the (001) faces of freshly cleaved single crystal, NaCl, KCl, and KBr. Tapping mode AFM studies of these materials show that their crystalline motifs vary widely depending upon the substrate and growth conditions and that a form of layered growth is observable in the first few monolayers of deposition for both dyes. Nucleation of these crystalline deposits at edge sites on these substrates appears to be central to the growth of the first monolayers of these materials. Luminescence spectra for both PTCDA and C4-PTCDI, captured in situ during the growth of the first 1–4 monolayers of material, show the presence of a monomer-like entity during the initial growth stage. For PTCDA thin films this luminescence signal decays rapidly as nucleation of the crystalline film occurs. As film coverage is increased, luminescence of ultrathin films of both dyes is dominated by emission from one or more excimeric states. For C4-PTCDI/KCl (001) the monomer-like emission does not completely disappear during the first monolayers of film growth, suggesting a degree of disorder sustained on a distance scale of a few molecular units at the grain boundaries and edges of the crystalline regions. The relative ratio of monomer/excimer emission of C4-PTCDI on KCl (001) is strongly temperature dependent and changes reversibly as the temperature is cycled between room temperature and 100 °C. The luminescence intensity for thin films of both dyes on all of the substrates investigated is enhanced in the presence of atmospheric oxygen, consistent with previously reported declines in the dark conductivity of these materials as they are taken from UHV to atmospheric environments.

## Introduction

Epitaxial growth of ultrathin films of various organic dyes often leads to new opportunities for study and optimization of their optical and electronic properties. Ordered thin-film growth of 3,4,9,10-perylenetetracarboxylicdianhydride (PTCDA) and *N,N*'-di-*n*-butylperylene-3,4,9,10-bis(dicarboximide) (C4-PTCDI, Figure 1) has recently been demonstrated on a variety of substrates, emphasizing in some instances the formation of close-packed monolayers that precede the growth of thicker films, and in other instances the crystal-

lography of multilayer films.<sup>1</sup> These perylene dyes are of importance in various technologies that utilize their solid-state absorbance and photoconductive properties.<sup>2–5</sup> Thin films of these dyes have tended to show an “*n*-type molecular semiconductor” electrical and photoelectrochemical response in single-layer and multilayer photovoltaic applications.<sup>4,6</sup> This electrical response, believed to arise from impurity doping of these thin films, is related to their relatively high electron affinity and stands in contrast to the “*p*-type” behavior seen for various phthalocyanine films that have often been

\* To whom correspondence should be addressed.

† Universität Bremen.

‡ University of Arizona.

§ Technische Universität Dresden.

(1) (a) Möbus, M.; Karl, N.; Kobayashi, T. *J. Cryst. Growth* **1992**, *116*, 495. (b) Tsuchida, A.; Hayashi, S.; Schnurpfeil, G.; Ashida, A.; Wörhle, D.; Yanagi, H. *Chem. Funct. Dyes* **1993**, *2*, 775. (c) Schmidt, A.; Schuerlein, T. J.; Collins, G. E.; Armstrong, N. R. *J. Phys. Chem.* **1995**, *99*, 11770. (d) Schmitz-Hübsch, T.; Fritz, T.; Sellam, F.; Staub, R.; Leo, K. *Phys. Rev. B* **1997**, *55*, 7972–7976. (e) Seidel, C.; Awater, C.; Liu, X. D.; Ellerbrake, R.; Fuchs, H. *Surf. Sci.* **1997**, *371*, 123. (f) Hoshino, A.; Isoda, S.; Kurata, H.; Kobayashi, T. *J. Appl. Phys.* **1994**, *76*, 4113. (g) Forrest, S. R.; Burrows, P. E.; Haskal, E. I.; So, F. F. *Phys. Rev. B* **1994**, *49*, 11309. (h) Hirose, Y.; Forrest, S. R.; Kahn, A. *Phys. Rev. B*; **1995**, *52*, 14040. (i) Umbach, E.; Sokolowski, M.; Fink, R. *Appl. Phys. A* **1996**, *63*, 565. (j) Seo, D.-K.; Ren, J.; Whangbo, M.-H. *Surf. Sci.* **1997**, *370*, 252.

(2) (a) Graser, F.; Hädicke, E. *Liebigs Ann. Chem.* **1980**, *1994*; **1984**, 483. (b) Graser, F.; Hädicke, E. *Acta Crystallogr.* **1986**, *C42*, 189, 195. (c) Klebe, G.; Graser, F.; Hädicke, E.; Berndt, F. *Acta Cryst.* **1989**, *B45*, 69.

(3) (a) Kazmaier, P. M.; Hoffman, R. *J. Am. Chem. Soc.* **1994**, *116*, 9684. (b) McKerrow, A. J.; Buncel, E.; Kazmaier, P. M. *Can. J. Chem.* **1993**, *71*, 390. (c) Debe, M. K.; Poirier, R. J. *J. Vac. Sci. Technol. A* **1994**, *12*, 2017.

(4) (a) Ferrere, S.; Zaban, A.; Gregg, B. A. *J. Phys. Chem.* **1997**, *101*, 4490. (b) Gregg, B. A. *J. Phys. Chem.* **1996**, *100*, 852. (c) Gregg, B. A. *Appl. Phys. Lett.* **1995**, *67*, 1271. (d) Gregg, B. A.; Sprague, J.; Peterson, M. W. *J. Phys. Chem.* **1997**, *101*, 5362. (e) Toda, Y.; Yanagi, H. *Appl. Phys. Lett.* **1996**, *69*, 2315. (f) Ohmori, U.; Tada, N.; Yashida, M.; Fujii, A.; Yoshino, K. *J. Phys. D, Appl. Phys.* **1996**, *29*, 2983. (g) Ostrick, J. R.; Dodabalapur, A.; Torsi, L.; Lovinger, A. J.; Kwock, E. W.; Miller, T. M.; Galvin, M.; Berggren, M.; Katz, H. E. *J. Appl. Phys.* **1997**, *81*, 6804–6807.

(5) Law, K.-Y. *Chem. Rev.* **1993**, *93*, 449.

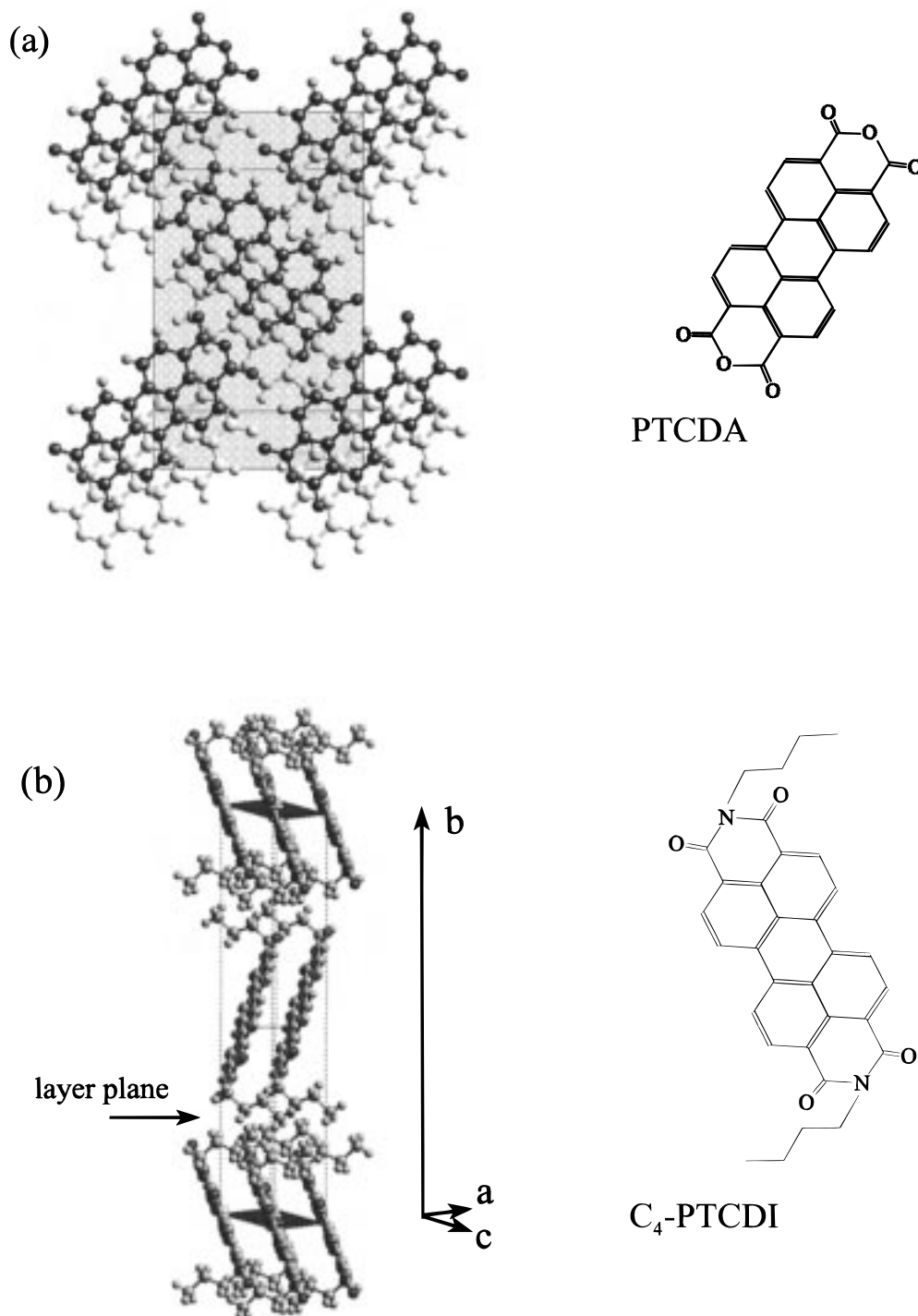


**Figure 1.** Schematic views of (a) the top view of the (102) plane of the PTCDA bulk structure (2 molecular layers of the  $\alpha$ -polymorph are shown, the anticipated growth direction from the surface is toward the reader) and (b) the C<sub>4</sub>-PTCDI bulk structure, with the *ac* plane parallel to the substrate, showing an anticipated growth direction along the *ab* axis direction, which achieves layer-by-layer growth.

interfaced to these perylenes.<sup>4,6</sup> Recent studies of PTCDA multilayer thin films, however, suggest strong anisotropies in conduction (p-type vs n-type), depending upon whether conduction is measured perpendicular or parallel to the molecular plane.<sup>4g</sup> Photovoltaic perylene/phthalocyanine bilayer thin films, capable of generating open-circuit photovoltages of several hundred millivolts, have been routinely created,<sup>6</sup> and these bilayers are of interest as efficient charge generation layers in a variety of emerging technologies. Creation of new, well-defined perylene/phthalocyanine heterojunctions, ordered on the molecular layer level, requires that both materials

deposit in "layer-by-layer" growth modes, forming conformal, pinhole-free thin films.

Several recent studies of epitaxial layer growth of crystalline organic films have suggested that, if one of the stable bulk structures of the material possesses close-packed layer planes which can be oriented parallel to a substrate plane, layered growth of this material is possible, under optimized deposition conditions.<sup>7,8</sup> Other factors that must be considered include (a) the strength of the interactions between the molecules in the first deposited monolayers and the atomic or molecular sites in the substrate, (b) the matching of unit-cell dimensions

in the overlayer with even multiples of the surface unit cell, to form either commensurate or coincident lattice superstructures, and (c) the possibility that ledge sites on the substrate, separating terraces, can act as nucleation sites for the first deposited material ("ledge-directed epitaxy").<sup>9,10</sup>

We report here the crystalline motifs observed for both PTCDA and C4-PTCDI on freshly cleaved NaCl (001), KCl (001), and KBr (001). The alkali halide single-crystal surfaces lend themselves to a comprehensive spectroscopic characterization of these thin films, including visible wavelength absorbance and luminescence and measurement of the dichroism of certain key infrared vibrations,<sup>11</sup> and provide opportunities for similar study of these phenomena in thin films of other classes of electroluminescent materials.<sup>12</sup> In this paper we evaluate the evolution of monolayer films toward "layered growth" modes for PTCDA and C4-PTCDI. C4-PTCDI belongs to a series of perylenebis(dicarboximide) dyes whose substituent chains greatly alter the types of possible crystal packing motifs,<sup>2</sup> leading to differences in their solid-state optical and electrical properties.

Transmission electron microscopy (TEM) studies of ca. 20 nm thick films of PTCDA on freshly cleaved NaCl (001) and KCl (001) surfaces have previously been observed to exhibit epitaxial growth.<sup>1a</sup> Both the  $\alpha$  and  $\beta$  phases of PTCDA have been observed on NaCl (001) and KCl (001), at several different azimuthal rotation angles of the PTCDA unit cell. For both polymorphs the (102) plane of the bulk unit cell lies parallel to the substrate (Figure 1a shows a top view of the (102) plane, showing two layers of the  $\alpha$ -polymorph). We confirm here layered growth of much thinner films of PTCDA on NaCl (001), KCl (001), and KBr (001) and discuss their possible epitaxial relationships with these surfaces. Luminescence spectra collected during the initial stage of film growth on substrates held at room temperature suggest the presence of isolated monomers of PTCDA, which disappear shortly following deposition of the first monolayer. These monomer-like emission

features are missing completely in thicker PTCDA films, as evidenced by the change in line shape of the spectra with coverage. Similar monomer-like emission spectra have been recently reported for very low coverages of PTCDA on quartz, at 10 K.<sup>13</sup> In that study the monomer-like emission features disappear upon warming to 100 K and were never observed at room temperature.

Previous TEM studies of the C4-PTCDI system have shown the possibility for crystalline motifs in films of 10–100 nm thickness in which the plane of the perylene dye does not lie parallel to the substrate<sup>1b</sup> (Figure 1b;  $a = 0.473$  nm,  $b = 2.823$  nm,  $c = 0.940$  nm; monoclinic unit cell,  $\beta_{ac} = 110.86^\circ$ ).<sup>2</sup> The close-packed ac layer plane was found to lie parallel to the KCl (001) substrate instead. On the macroscopic scale C4-PTCDI films appear to be more conformal to the substrate than PTCDA films. We see quite different crystalline motifs for these thin films on all three alkali halide surfaces and a much stronger persistence of the monomer-like luminescence spectrum in the case of C4-PTCDI films deposited on KCl substrates.

For both molecules, nucleation of the crystalline thin film is strongly influenced by edge-sites and terraces on the freshly cleaved salt surfaces. AFM images of C4-PTCDI films, taken after deposition of the first 1–3 monolayers, demonstrate the tendency for these molecules to transition from flat-lying monomers toward aggregate motifs more reminiscent of the bulk structure.

## Experimental Section

All thin films were grown under high vacuum conditions in growth chambers similar to those previously described.<sup>1c,7a,14</sup> Evaporation occurred from Knudsen cell sublimation sources, and film thickness was estimated from a quartz crystal microbalance. Substrate temperatures were controlled by conventional resistive heating of the sample stage and monitoring with a thermocouple attached to a molybdenum plate to which the alkali halide crystals were attached via spring clips. Alkali halide single crystals (Commercial Crystal Laboratories; Garfield, NJ) were freshly cleaved before each experiment (samples were typically  $1 \times 1$  cm and 1–2 mm in thickness) and immediately inserted into the vacuum system, where they were held at temperatures of either ca. 100 or ca. 250 °C overnight. Differences in cleaving techniques and annealing of these crystals in the vacuum chamber could produce wide variations in the number and width of terraces in these surfaces.<sup>11</sup> Rapid cleaving conditions (by striking the crystal with a razor edge) and lower annealing temperature left large terraces (widths of up to 10  $\mu$ m) on the surfaces of the crystals, with clearly defined boundaries (step edges) running parallel to the major crystallographic axes of the alkali halide crystal. Slow cleavage (by using steady, slow pressure from the razor edge) and higher annealing temperatures generally produced narrower, more plentiful, and highly faceted terraces, such that no clear orientation versus the substrate major axes were observable. Both types of substrates are shown in this paper.

The OMBE deposition chamber was modified to allow for folding of the modulated 488 nm line (ca. 10 mW, 1 kHz modulation) of an argon ion laser (Ion Laser Technologies) into the chamber through a quartz viewport. The excitation source

(6) (a) Meyer, J.-P.; Schlettwein, D.; Wörhle, D.; Jaeger, N. *Thin Solid Films* **1995**, *258*, 317. (b) Schlettwein, D.; Armstrong, N. R.; Lee, P. A.; Nebesny, K. W. *Mol. Cryst. Liq. Cryst.* **1994**, *253*, 161. (c) Hiramoto, M.; Ihara, K.; Yokoyama, M. *Jpn. J. Appl. Phys.* **1995**, *34*, 3803. (d) Danziger, J.; Dodelet, J.-P.; Armstrong, N. R. *Chem. Mater.* **1991**, *3*, 812. (e) Tomizhinani, G.; Dodelet, J.-P.; Loté, R.; Gravel, D. *Chem. Mater.* **1991**, *3*, 1046. (f) Oekermann, T.; Schlettwein, D.; Wörhle, D. *J. Appl. Electrochem.*, in press. (g) Wörhle, D.; Kreinhoop, L.; Schnurpfeil, G.; Elbe, J.; Tennigkeit, B.; Hiller, S.; Schlettwein, D. *J. Mater. Chem.* **1995**, *5*, 1819. (h) Wörhle, D.; Kreinhoop, L.; Schlettwein, D. In *Phthalocyanines—Properties and Applications*; Leznoff, C. C., Lever, A. P. B., Eds.; New York, 1996; Vol. 4. (i) Tang, C. W. *Appl. Phys. Lett.* **1986**, *48*, 183. (j) Borsenberger, P. M.; Weiss, D. S. *Organic Photoreceptors for Imaging Systems*; Marcel Dekker: New York, 1993; pp 101–145.

(7) (a) Schmidt, A.; Chau, L.-K.; Back, A.; Armstrong, N. R. In *Phthalocyanines—Properties and Applications*; Leznoff, C. C., Lever, A. P. B., Eds.; New York, 1996; Vol. 4, pp 311–341, and references therein. (b) England, C. D.; Collins, G. E.; Schuerlein, T. *J. Langmuir* **1994**, *10*, 2748.

(8) (a) Hillier, A.; Ward, M. *Phys. Rev. B* **1996**, *54*, 14037. (b) Fritz, T.; Armstrong, N. R.; manuscript in preparation.

(9) Bonafede, S. J.; Ward, M. D. *J. Am. Chem. Soc.* **1995**, *117*, 7853.

(10) (a) Tiller, W. A. *The Science of Crystallization: Microscopic Interfacial Phenomena*; Cambridge University Press: New York, 1991; pp 171–199. (b) Lüth, H. *Surfaces and Interfaces of Solids*; Springer-Verlag: New York, 1993; pp 94–114.

(11) (a) Back, A. Ph.D. Dissertation, University of Arizona, 1997. (b) Back, A.; Armstrong, N. R.; Schlettwein, D.; Schilling, B., manuscript in preparation.

(12) Schilling, B.; Armstrong, N. R., manuscript in preparation.

(13) Gómez, U.; Leonhardt, M.; Port, H.; Wolf, H. C. *Chem. Phys. Lett.* **1997**, *268*, 1.

(14) (a) England, C. D.; Collins, G. E.; Schuerlein, T. J.; Armstrong, N. R. *Langmuir* **1994**, *10*, 2748. (b) Schmidt, A.; Schlaf, R.; Louder, D.; Chau, L.-K.; Chen, S.-Y.; Fritz, T.; Lawrence, M. F.; Parkinson, B. A.; Armstrong, N. R. *Chem. Mater.* **1995**, *7*, 2127.

impinged on the sample at an angle of ca.  $45^\circ$  to the substrate normal, and the luminescence signal was outcoupled through a sapphire viewport and collection optics at an angle of ca.  $45^\circ$  to the surface normal, so that the planes defined by the excitation beam and the detection optics were perpendicular to each other. This outcoupled light was then passed through a J-Y H-20 monochromator, coupled to a Hamamatsu R446 photomultiplier. The signal from the PMT was read with a EG&G 5209 lock-in-amplifier locked to the 1 kHz modulation frequency of the excitation laser. Further details of this chamber and the optics necessary to examine this luminescence will be published elsewhere.<sup>11</sup>

Following deposition, the films were withdrawn from the deposition chamber and subjected to further spectroscopic and tapping-mode (in air) AFM characterization. AFM analysis was performed with a Nanoscope III (Digital Instruments) in tapping mode using oxide-sharpened silicon nitride tips. In most cases the samples were placed in the AFM housing in such a way as to allow for scanning of the tip parallel to a principal crystallographic axis of the substrate, so as to conveniently allow for determination of the growth directions of the perylene crystals. Resolution of images down to an  $x,y$  distance scale of  $0.1 \mu\text{m}$  was achievable, but the weakness of the interaction between the overlayer and the substrate has, to date, prevented acquisition of good-quality molecular resolution images.

## Results and Discussion

**AFM Studies.** Figures 2 and 3 show tapping-mode AFM images on the 3–5  $\mu\text{m}$  distance scale of crystalline deposits of the two perylene dyes, on all three alkali halide surfaces, at coverages of ca. 2–10 equivalent monolayers. Deposition temperatures for these studies were generally kept in two regimes, below ca.  $40^\circ\text{C}$  and between 90 and  $110^\circ\text{C}$ . For PTCDA, deposited in the lower temperature regime, small rectangular, platelike crystallites were observed on all three substrates (not shown), with the long axes of the organic crystal aligned ca.  $45^\circ$  to the principal axes of the substrate crystal. These images suggest that nucleation of these crystallites occurs along the plentiful step edges in the substrate.

PTCDA deposited in the higher temperature regime, on NaCl (001) (Figure 2a,b) shows crystalline motifs that are strongly reminiscent of those seen for much thicker films reported earlier and assigned through TEM (electron diffraction) analysis to the  $\alpha$  and  $\beta$  polymorphs of the stable bulk structure of PTCDA.<sup>1a</sup> [Dimensions proposed for the unit cells for these two polymorphs are similar;  $\alpha$  polymorph:  $b_1 = 1.196 \text{ nm}$ ,  $b_2 = 1.998 \text{ nm}$ ,  $\beta = 90^\circ$ ;  $\beta$  polymorph:  $b_1 = 1.245 \text{ nm}$ ,  $b_2 = 1.930 \text{ nm}$ ,  $\beta = 90^\circ$ ; the  $\alpha$  and  $\beta$  polymorphs differ in the translations ( $\alpha =$  long crystallographic axis,  $\beta =$  short axis) of the second layer of PTCDA with respect to the first layer].<sup>1a</sup>

Nucleation of the deposits occurs at the larger step edges of the NaCl surface, and follows a dendritic growth pattern, with each dendrite appearing to grow along one direction until intersection with another step edge. Changes of direction of the growing crystallites occurred along  $60$  and  $120^\circ$  angles, consistent with the angle between the  $[010]$  and  $[-201]$  directions (i.e., the diagonal along the unit cell of the PTCDA (102) plane). We have also occasionally seen crystallites which clearly intersected a step edge and grew another layer of PTCDA so that the step edge was completely covered by this crystallite.<sup>11</sup> Line scans taken along the top surface of these crystallites show them to be flat to

$\pm 0.05 \text{ nm}$  with large terraces of up to  $0.5 \mu\text{m}$  in diameter separated from the adjacent terraces by steps with a height of  $0.4 \pm 0.1 \text{ nm}$  (see inset, Figure 2a). These step heights correspond to, within the uncertainty of this measurement, the thickness of one flat-lying layer of PTCDA.

On several samples, scans taken *between* these larger crystallites show the alkali halide substrate to be covered nearly uniformly with an additional thin layer, whose occasional pinholes allowed determination of its thickness ( $0.3\text{--}0.4 \text{ nm}$ ). Since such thin films with occasional pinholes are not seen on the bare substrate, we conclude that a flat-lying monolayer of PTCDA initiates growth on this surface. This observation has been recently confirmed for a number of the perylene dyes, and is reflected in the wavelength for monomer-like emission seen in these material (see below). Preliminary reflection high-energy electron diffraction (RHEED) data, taken during the initial monolayer deposition of PTCDA on these surfaces, is consistent with a flat-lying orientation of the first deposited monolayer, as has been observed in the growth of PTCDA on numerous other substrates such as Au(111), HOPG, etc.<sup>1d,f,g</sup>

On KBr and KCl surfaces (Figure 2c,d) higher temperature growth conditions lead to larger PTCDA crystallites, which exhibit less dendritic growth than is observed on the NaCl surfaces. The KBr and KCl surfaces shown here were subjected to the lower temperature anneal cycle before PTCDA deposition, leaving  $1/2$ -unit-cell height steps, with terraces that are uniform over micron distance scales. Each of the PTCDA crystallites observed on these terraces is layered, as before, with clear indications of uniform thickness over micron distance scales. Occasional steps down to lower thicknesses were observed, where the step height varied from  $0.4 \text{ nm}$  (single monolayer (ML)) to multiples of several monolayer units. The orientation of the long axes of these larger crystallites on KBr appears to correspond approximately to the principal axes of the alkali halide substrate, while on KCl, an orientation of ca.  $\pm 20^\circ$  is observed.

Figure 3 summarizes the crystalline deposits seen for C4-PTCDI thin films on the (001) faces of these salt crystals. On NaCl (001) deposition of a 2 ML thick film at ca.  $75^\circ\text{C}$  leads to the growth of very high aspect ratio thin crystals, which have a consistent orientation with respect to the substrate, as shown in Figure 3a. On this same substrate, in the lower temperature growth regime, similar deposits were observed, but with much shorter needlelike crystallites. The dimensions of the individual crystals in Figure 3a are ca.  $10\text{--}150 \text{ nm}$  in width,  $4\text{--}14 \text{ nm}$  in height, and up to  $0.5 \mu\text{m}$  in length. The long axis of each organic crystal is aligned ca.  $\pm 10^\circ$  with respect to the principal axes of the substrate unit cell. Careful examination of these thin films, in the regions between the larger crystallites, showed additional uniform layers, with some pinhole defects that were ca.  $0.4 \pm 0.1 \text{ nm}$  deep, consistent with the idea

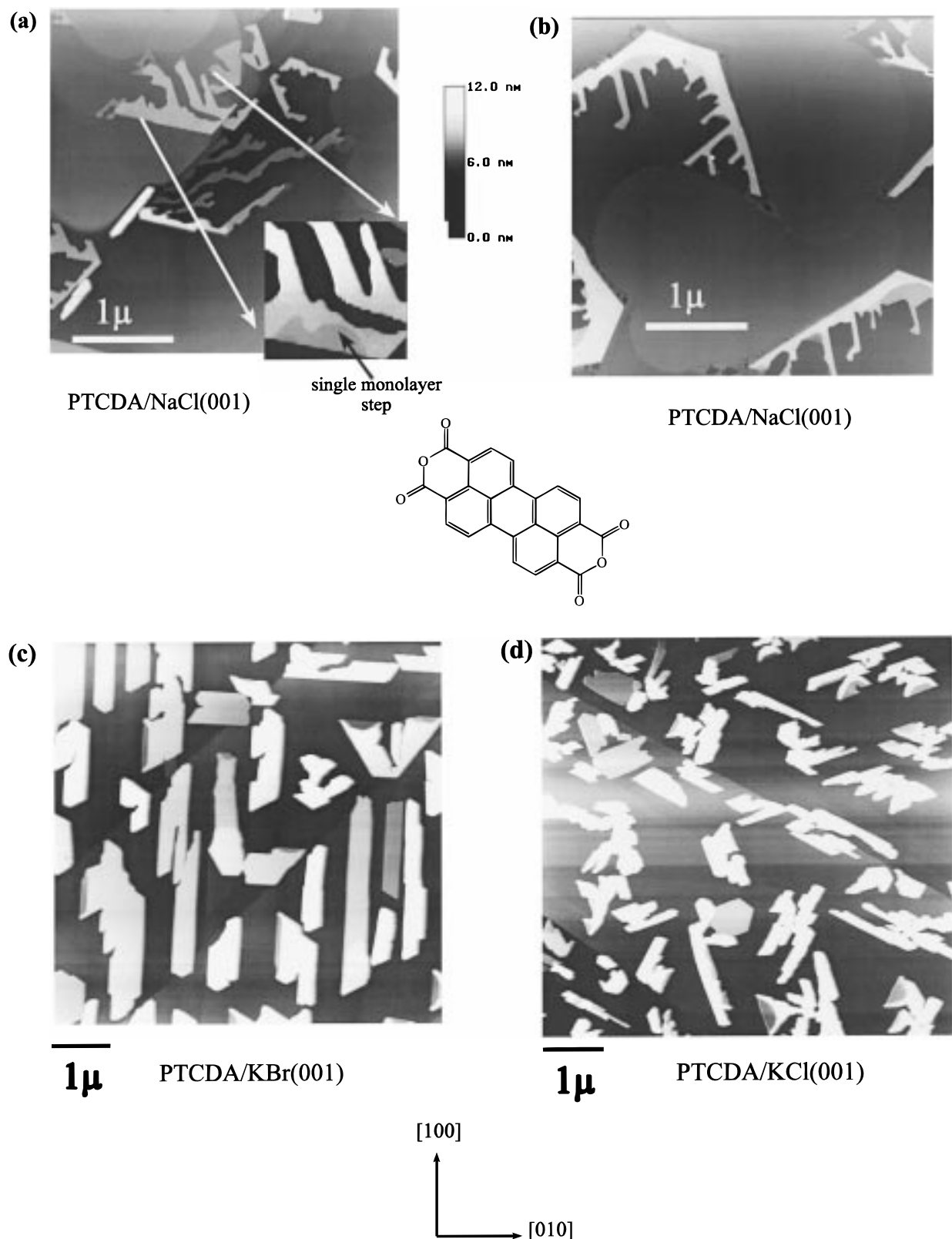


**Figure 2.** AFM images of ca. 1–2 equivalent monolayer coverages of PTCDA on (a and b) NaCl(001), (c) KBr(001), and (d) KCl(001). Single molecular steps are observable in (a) on the planes of the PTCDA crystallites, and additional multimolecular height steps are indicated on some of the other crystallites.

that the first deposited material forms a flat-lying monolayer, similar to the growth of PTCDA on these surfaces. Under these growth conditions it is apparent that the intermolecular interactions within the perylene deposit lead to layer-plus-island (SK) growth.<sup>10</sup> The registry of the larger crystals with the substrate mate-

rial suggests that the first deposited material is also ordered with respect to the substrate and that the subsequent high aspect ratio crystals grow out of, or next to, this first ordered layer.

Low-temperature growth conditions (ca. 36 °C), on KCl and KBr surfaces, produce structures such as those

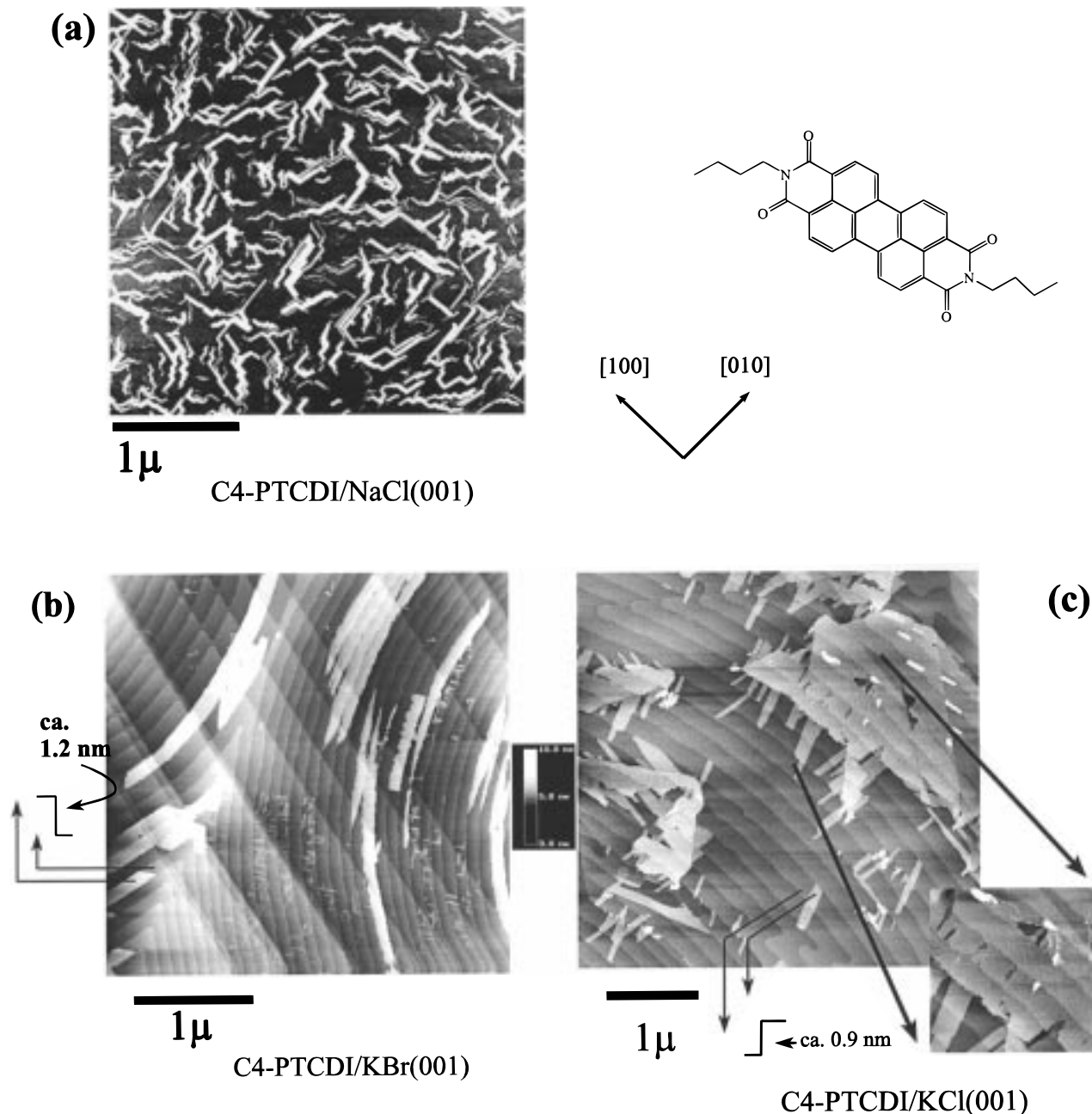


**Figure 3.** AFM images of ca. 1–2 equivalent monolayer coverages of C4–PTCDI on (a) NaCl(001), (b) KBr(001), and (c) KCl(001). In (a) the crystallites tend to average 4–6 nm in height, 10–150 nm in width, as with PTCDA above. The highly stepped KBr and KCl surfaces show terraces on the bare surface separated by steps that are a half-unit cell in height (0.33 nm for KBr and 0.315 nm for KCl). The thickness for a single layer of perylene dye on these surfaces is also shown.

shown in Figure 3b,c for submonolayer coverages of C4–PTCDI. In these cases it is interesting to note that crystalline deposits conform closely to the terraces on the substrate (heavily stepped surfaces, prepared by a high-temperature annealing cycle, have been chosen for viewing here, with each step on the bare substrate corresponding to the thickness of half of the unit cell of either KBr (0.33 nm) or KCl (0.32 nm)). On the KCl surfaces especially, we typically observe crystal growth that not only conforms to an entire terrace width but also spans several terraces, with the fluctuation in height of the perylene deposit corresponding to the fluctuation in height of the substrate. This growth pattern is sustained as these films increase in coverage, eventually leading to a reasonably conformal, defect-free thin film.

Individual dye layer thicknesses were determined by AFM to be ca. 1.2–1.4 nm on the KBr substrate and 0.8–1.0 nm on the KCl substrate. For C4–PTCDI on KBr (001) this thickness is consistent with an orientation in the first monolayer with the  $a$ – $c$  plane parallel to the substrate (perylene cores oriented as shown in Figure 1b), with a half-unit-cell height (one close-packed monolayer) of ca. 1.4 nm.<sup>1b,2</sup> For C4–PTCDI on KCl the thin film thickness is consistent with an orientation of the  $a$ – $b$  plane down, with a unit cell thickness of ca. 0.94 nm, which is not consistent with previous TEM studies of much thicker films on KCl.<sup>1b</sup> The extent to which these morphological differences are adhered to as film coverage increases is under investigation using the anisotropies seen in the visible absorbance and infrared bands of these materials.<sup>11</sup>

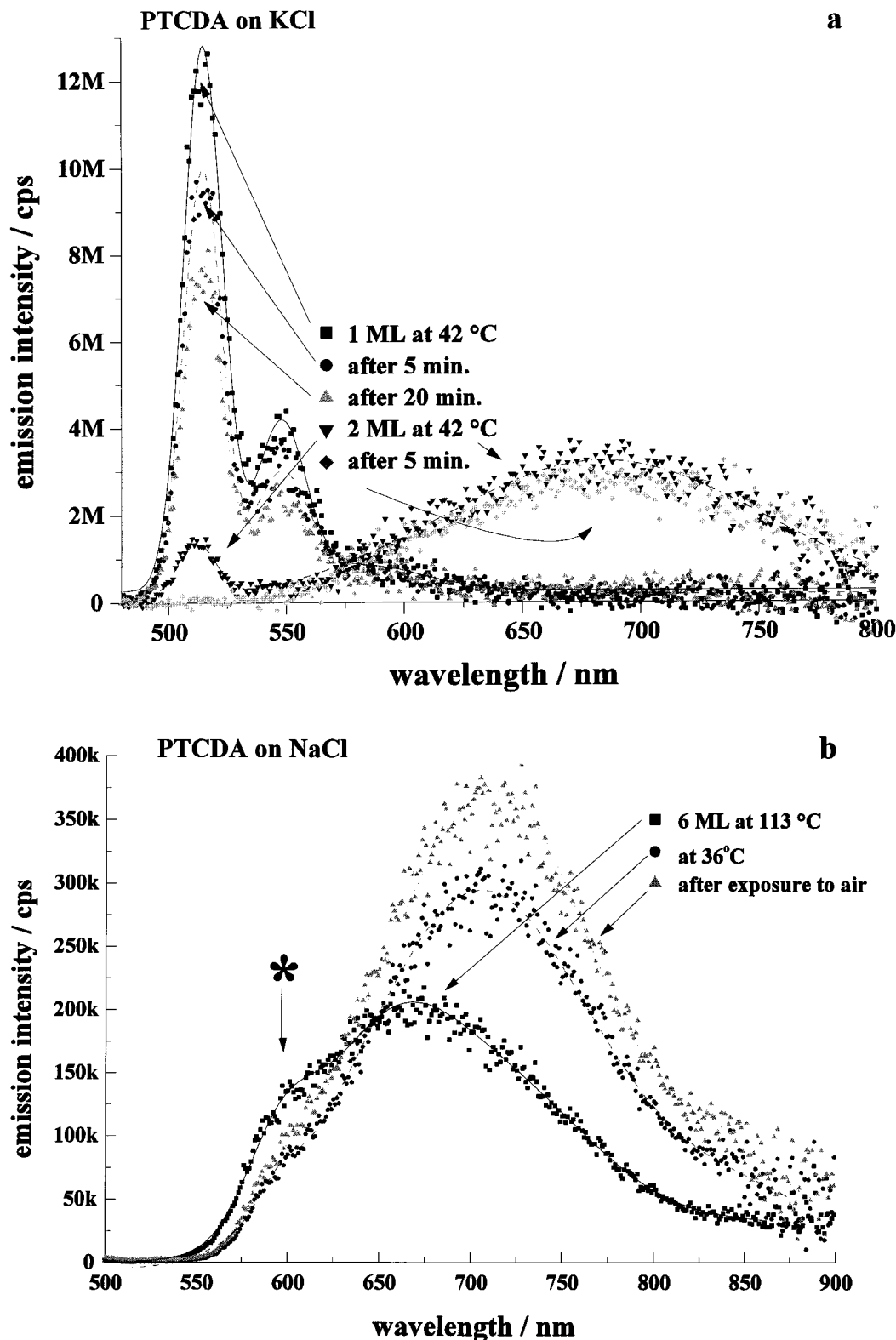


**Figure 4.** Luminescence spectra for 1–2 ML coverages of PTCDA on (a) KCl(001) and (b) NaCl(001). The monomer-like emission can be seen for 1 ML coverages (and below) and decays quickly upon sitting at near room temperature. The emission signal at ca. 680 nm grows in at higher PTCDA coverages. The intensity of the higher energy emission shoulder (seen here for the PTCDA/NaCl system) relative to the rest of the emission spectrum was strongly temperature dependent.

**In Situ Luminescence Studies.** The luminescence spectra of these perylene dyes, captured in situ during their deposition, provide complementary information about the morphological transitions occurring during the formation of the first few monolayers of the thin film, probed over a spectroscopic length scale of a few

molecular units.<sup>13,15</sup> The extremes in luminescence behavior observed for these thin films are shown in Figures 4 and 5, which are typical of samples subsequently leading to the AFM images shown above.

The first deposited submonolayer to monolayer coverages of PTCDA films on all substrates exhibit monomer-

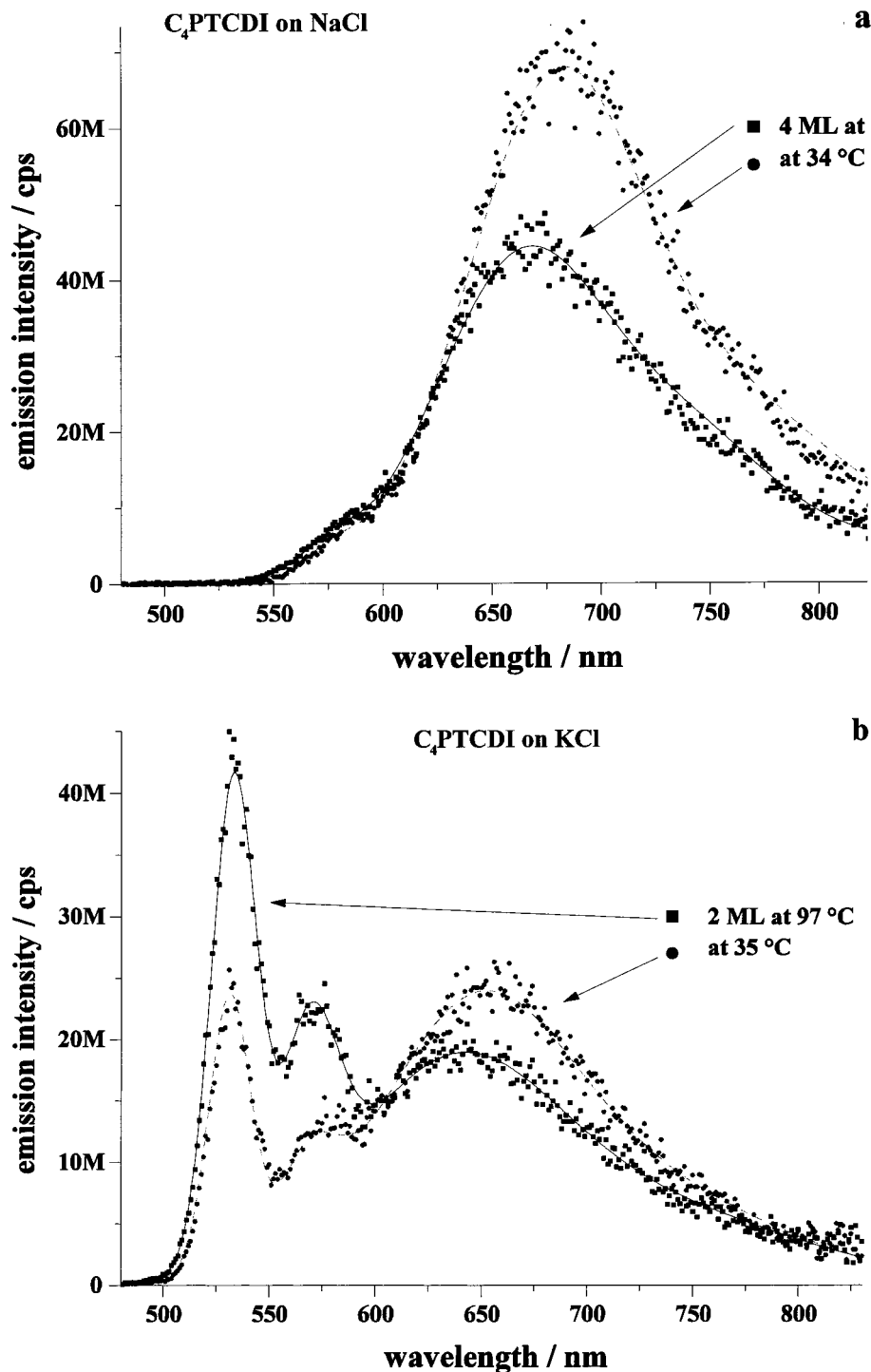


**Figure 5.** Luminescence spectra for C<sub>4</sub>-PTCDI on (a) NaCl(001) and (b) KCl(001). The monomer emission signal for this perylene on KCl was strong and persistent and could be reversibly decreased and increased in intensity by cycling the temperature up (97 °C is shown) and down (35 °C is shown). For this same perylene dye on NaCl, where only dendritic island growth was observed, only the excimer luminescence signal was observed at multilayer coverages.

like emission signals, with luminescence maxima at 520–525, 550, and ca. 590 nm, as shown for PTCDA on KCl (001) in Figure 4a. These features closely mimic the luminescence spectra of dilute chloroform solutions of both PTCDA and several perylenebis(dicarboximides) (such as C<sub>4</sub>-PTCDI) but are blue-shifted by ca. 20 nm from their solution spectra, due to the strength of the interaction of the core of the dye molecule with the substrate material.<sup>1a,11</sup> We have recently been able to correlate the strength of interaction of the first deposited

molecules in a series of these perylene dyes with alkali halide or glass surfaces, by comparison of the position of the luminescence spectral response of monomer features on these surfaces versus those for the monomer in a chloroform solution. A blue shift in this response is seen (ca. 10–20 nm) for PTCDA on all of the alkali halides and for the C<sub>4</sub>-PTCDI system on KCl (001). For C<sub>4</sub>-PTCDI, the spectral response on both NaCl and KBr surfaces is essentially the same as seen for dilute chloroform solutions, suggesting a weaker interaction



with these substrates. The luminescence behavior of low coverages of PTCDA on silica (quartz) surfaces has been recently reported, where this monomer-like emission could only be sustained by keeping the system at 10 K.<sup>13</sup> The length of time that we are able to sustain these monomer-like emission features, especially on KCl, suggests that the interaction of the dye with the alkali halide surface may help to stabilize this monomeric entity.

If deposition is stopped at a coverage of ca. 1 ML, even near room temperature, there is a steady decline in luminescence intensity in this spectral region over the space of several seconds to minutes, with no detectable increase in the intensity of longer wavelength emission bands. The rate of decay of this monomer emission feature appears to increase with increasing surface coverage of PTCDA, up to coverages of 1 ML, indicating that the decline in emission intensity is directly related to the rate of interaction of mobile species on the alkali halide surface. As coverage is increased to 2 monolayers, a new broad luminescence band centered at ca. 680 nm intensifies, which we attribute to excimeric emission.<sup>15,16</sup> These results suggest that the first deposited material experiences only weak intermolecular interactions, which allow monomer-like environments for luminescence. The longer wavelength emission band only arises when the surface coverage is sufficient to initiate nucleation of the deposited material into stable, bulklike cofacial crystal architectures.

It is clear from these studies that the luminescence probability for the monomer-like emission is higher by a factor of *at least* 10 $\times$  than for the excimeric emission, since the monomer signal is completely attenuated for thin films that are monolayer-to-bilayer in coverage (as seen in the AFM data), with only small levels of detectable emission from the excimeric state. The relative intensity of monomeric versus excimeric emission spectra is known to be sensitive to intermolecular interactions over a distance scale involving two adjacent molecules and the group of molecules that are at the van der Waals approach distance to this pair and is therefore an indicator of short-range ordering in these thin films.<sup>13,15,16</sup>

As the coverage is increased from ca. 2 to 20 monolayers, the emission spectrum due to the aggregate in these PTCDA films continues to red-shift from 680 nm at the lowest coverage to 710 nm for the highest coverages, which is within 5 nm of the emission band seen for the bulk material (as shown in Figure 4b). This progressive red-shift in the luminescence band is expected if the excitonic interactions build progressively

over 10–20 monolayer coverages, as has been seen in other epitaxial and polycrystalline thin-film organic dyes.<sup>13–18</sup> For depositions in the high-temperature regime, the peak emission from the excimer band, recorded while the sample was held at the growth temperature (e.g., 110 °C in Figure 4b), was blue-shifted by ca. 40 nm (670 vs 710 nm), relative to the position of this band near room temperature. This blue-shifting of emission with increasing temperature is also characteristic of excimer formation.<sup>16</sup>

The high-energy shoulder on the emission band in Figure 4b at ca. 590 nm (\* in Figure 4b) is seen at 2–6 monolayer coverages. Above ca. 6 monolayers this spectral feature is absent, indicating that this luminescence peak arises from an interaction specific to the formation of the second layer of material that is not sustained as thicker films are formed (e.g., a kind of phase boundary between the first and subsequent layers, arising from lattice strain between the first and second layer). This spectral feature has also been seen for the formation of certain epitaxial PTCDA layers on Au (111) surfaces.<sup>19</sup> Similar behavior has also been recently observed for luminescence studies of vacuum-deposited liquid-crystalline biphenyls<sup>20</sup> and is characteristic of “Y-type” excimers in other perylene thin films and glasses. We believe these “Y-type” excimers are due to intermediate structures that evolve into the final cofacial dimer aggregate, from which “E-type” excimer emission (the longest wavelength emission band) is observed.

For C4–PTCDI films on NaCl and KBr behavior very similar to that noted above for PTCDA films was observed, as seen in Figure 5a. At low coverages, monomer-like emission spectra were observed, which gave way to emission from excimer states as the coverage increased. As for PTCDA films, the energy of the excimeric emission was blue-shifted when observed at higher temperatures. The wavelength maxima for emission response for this monomeric feature on both of these substrates were virtually unchanged with respect to solution spectra of the monomer species.

In contrast, for C4–PTCDI on KCl (001) (Figure 5b) the monomer-like signal persists as coverage is increased to well above monolayer levels, even at deposition temperatures as high as 110 °C. The monomer-like spectra at the lowest coverages of dye were also blue-shifted by ca. 10–15 nm, suggesting a stronger interaction of this dye with the KCl surface versus the other two alkali halides. In a film deposited at this elevated temperature, subsequent lowering of the substrate temperature to ca. 35 °C leads to a decrease in the intensity of the monomer-like emission feature and an increase in intensity and red-shift of the emission due to the aggregated molecules (640 nm at 97 °C to 660 nm at 35 °C). Interestingly, this process was partially reversible if the temperature was raised and then lowered again, suggesting that the small portions

(15) (a) Saigusa, H.; Lim, E. C. *Acc. Chem. Res.* **1996**, *29*, 171. (b) Walker, B.; Port, H.; Wolf, H. C.; *Chem. Phys.* **1985**, *92*, 177. (c) Weiss, D.; Kietzmann, R.; Mahrt, J.; Tufts, B.; Storck, W.; Willig, F. *J. Phys. Chem.* **1992**, *96*, 5320. (d) Mahrt, J.; Willig, F.; Storck, W.; Weiss, D.; Kietzmann, R.; Schwarzburg, K.; Tufts, B.; Trösken, B. *J. Phys. Chem.* **1994**, *98*, 1888. (e) Komfort, M.; Löhmansröben, H.-G.; Salthammer, T. *J. Photochem. Photobiol. A* **1990**, *51*, 215. (f) Vitukhnovsky, A. G.; Sluch, M. I.; Warren, J. G.; Petty, M. C. *Chem. Phys. Lett.* **1990**, *173*, 425. (g) Vitukhnovsky, A. G.; Sluch, M. I.; Warren, J. G.; Petty, M. C. *Chem. Phys. Lett.* **1991**, *184*, 235. (h) Hoffman, M.; Böttcher, H. *J. Fluor.* **1995**, *5*, 217. (i) Bulovic, V.; Burrows, P. E.; Forrest, S. R.; Cronin, J. A.; Thompson, M. E. *Chem. Phys.* **1996**, *210*, 1. (j) Haskal, E. I.; Shen, Z.; Burrows, P. E.; Forrest, S. R. *Phys. Rev. B* **1995**, *51*, 4449. (k) Haskal, E. I.; Zhang, Z.; Burrows, P. E.; Forrest, S. R. *Chem. Phys. Lett.* **1994**, *219*, 325.

(16) (a) Birks, J. B.; Kazzaz, A. A.; King, T. A. *Proc. R. Soc. A* **1966**, *291*, 556. (b) Birks, J. B.; Kazzaz, A. A. *Proc. R. Soc. A* **1968**, *304*, 291.

(17) (a) Aroca, R.; Johnson, E.; Maiti, K. *Appl. Spectrosc.* **1995**, *49*, 467. (b) Johnson, E.; Aroca, R. *Appl. Spectrosc.* **1995**, *49*, 472. (c) Johnson, E.; Aroca, R.; Nagao, Y. *J. Phys. Chem.* **1991**, *95*, 8840.

(18) Chau, L.-K.; England, C. D.; Chen, S.-Y. *J. Phys. Chem.* **1993**, *97*, 2699.

(19) Schmitz-Hübsch, T.; Fritz, T.; Leo, K., manuscript in preparation.

(20) Itaya, A.; Watanabe, K.; Imamura, T.; Miyasaka, H. *Thin Solid Films* **1997**, *292*, 204.

of the film responsible for the monomer-like emission for the C4-PTCDI system are able to transition between ordered and disordered environments (a type of two-dimensional melting and recrystallization at the grain boundaries and edges of the crystallites in the growing thin films), as the temperature is cycled.

Of special note for these studies is the effect of venting the deposition system to atmosphere or oxygen. Figure 4b shows a representative luminescence spectra of a PTCDA film before and after venting of the system and is typical for most multilayer PTCDA and C4-PTCDI films examined to date. The adsorption of oxygen has been presumed to lead to quenching of luminescence in many aromatic dyes.<sup>21</sup> Instead of this behavior we saw *enhancement* of luminescence of both the monomer and excimer signal upon exposure to oxygen. From previous studies we have determined that the dark conductivity of these and similar perylene dye thin films is typically ca.  $10^{-5} \Omega^{-1} \text{cm}^{-1}$  as deposited, whereas after exposure to atmosphere this conductivity drops to ca.  $10^{-10} \Omega^{-1} \text{cm}^{-1}$ .<sup>6b</sup> The high dark conductivity in the as-deposited material is presumed to originate from impurity doping of these thin films, arising from the electron-acceptor character of these dyes. This electron-acceptor character has been revealed by a combination of UV-photoelectron spectroscopy and electrochemical studies, which allow estimation of the frontier orbital positions of these thin films versus vacuum.<sup>22</sup> Oxygen has been proposed to react with these electron-rich impurity centers, trapping the extra charge carriers and lowering the dark conductivity.<sup>6b</sup> This change in conductivity with atmospheric oxygen exposure is reversible, upon annealing in UHV or in the presence of a donor such as  $\text{NH}_3$ , the initial dark conductivity of these thin films is significantly restored. Such impurity dopants, if possessing a permanent charge or strong dipole, are predicted to act as exciton dissociation centers, as demonstrated by Popovic and co-workers for a range of perylene and phthalocyanine dyes.<sup>23</sup> The reaction of oxygen with these impurity sites would therefore be expected to enhance luminescence efficiencies while simultaneously lowering dark conductivity. It is reasonable that this effect can dominate the other losses in luminescence efficiency normally associated with the presence of adsorbed oxygen. Closer correlations of changes in dark and photoconductivities and changes in luminescence efficiency for a variety of these perylene dyes are underway.

### Conclusions

For the deposition of PTCDA on the alkali halide single-crystal surfaces, it is clear that layered growth is initiated in the first monolayers and that the interaction between molecules leads to rapid formation of the excimer state and loss of the monomer-like state in the luminescence of these molecules. The observation of emission from a monomer-like state at submonolayer coverages on the alkali halide surfaces (when no such

features are observable at these deposition temperatures on quartz or glass) confirms that interactions between the first monolayer and the substrate are important in controlling growth of such ultrathin films.<sup>11,13</sup>

The growth patterns that we see for PTCDA in the first few monolayers deposited on NaCl (001), as revealed by our AFM data, are striking in their similarity to the electron microscopy data for the much thicker films in ref 1a, and it would appear that there is continuity of crystalline motifs from monolayer to multilayer film thicknesses on this substrate, under comparable growth conditions.

For the C4-PTCDI system, however, it is clear that there is a transition occurring from a flat-lying molecular film toward the stable layered bulk structure, at coverages characterized here by both AFM and luminescence spectroscopies. The persistence of the monomer-like emission in this system is consistent with the small degree of disorder sustained in these crystallites as this transition is undertaken. The monomer-like luminescence signal probably occurs with at least a factor of  $10\times$  the probability for emission from the excimer states on the surface, suggesting that these emission spectra originate from a minority of molecules on the alkali halide surface. For both materials there is a clear tendency for the step edges in the alkali halide surfaces to act as nucleation sites for crystal growth, thereby controlling the morphology of the first deposited layers.

Without molecular resolution images of these perylene dyes on the alkali halide surfaces, it is difficult to suggest what the epitaxial relationship is between the first monolayer of dye and the substrate. Möbus et al. suggested orientations for the first deposited molecules for PTCDA on the NaCl (001) and KCl (001) surfaces, which maximize the interaction of the carbonyl oxygens of the flat-lying PTCDA molecule with the cation sites of the alkali halide (001) plane.<sup>1a</sup> In the case of the NaCl (001) surface, epitaxial relationships were proposed that place all four carbonyl oxygens over cation sites. In this orientation the center of the perylene core of the molecule lies over an anion site. This orientation was consistent with the observed azimuthal rotation of the  $\alpha$ -polymorph ( $\phi = 4^\circ$ ) and  $\beta$ -polymorph ( $\phi = 7^\circ$ ) with respect to the major crystallographic axes of the substrate. In the case of the KCl (001) surface, the increase in lattice dimension affords only the opportunity for two opposing carbonyl oxygens to be placed over cation sites in the surface, with an azimuthal rotation ( $\phi = 24^\circ$ ) for both  $\alpha$  and  $\beta$  forms of this material. Interestingly, in this case, such a rotation also places the center of the perylene core of this molecule directly over a cation site, which may increase the favorable interaction of these molecules with the KCl surface.<sup>11</sup> In the case of the KBr (001) surface, adsorption of the molecule with two opposing carbonyl oxygens adjacent to cation sites is also possible, but the separation distance between carbonyl oxygens and the surface cations is larger than for the KCl surface. This orientation also places the perylene core over a cation site, as for KCl. These authors acknowledge, and our experiments here tend to confirm, that such relationships between the first deposited molecules and the substrate may be sacrificed as the

(21) Lakowicz, J. R. *Principles of Fluorescence Spectroscopy*; Plenum Press: New York, 1983.

(22) Schmidt, A.; Anderson, M.; Schlettwein, D.; Armstrong, N. R. *J. Phys. Chem.*, submitted.

(23) (a) Popovic, Z. D. *J. Chem. Phys.* **1982**, *77*, 498. (b) Popovic, Z. D. *J. Chem. Phys.* **1983**, *78*, 1552.

film coverage increases, and intermolecular forces and/or ledge or edge-site directed nucleation and growth begins to dominate the azimuthal rotation of the resultant crystalline deposit.

In the case of the C4-PTCDI films we can anticipate similar relationships between a flat-lying perylene core and these substrates, provided that the butyl chains can be tilted away from the surface, or lie parallel to the surface, creating a more open monolayer structure than for PTCDA. Such flat-lying structures, however, represent a significant departure from the stable bulk structure of this material. This lattice strain, in those cases where the interaction with the substrate is weakest, is likely to be relieved early in the formation of the complete thin film, and one anticipates evidence of this in both the luminescence signals from such surfaces, as well as the AFM images (e.g., C4-PTCDI films on the NaCl (001) surface).

Experiments to be reported elsewhere show that by the time 20–60 monolayers of C4-PTCDI film have been deposited on these alkali halide single-crystal surfaces, perylene orientations have been achieved that may be consistent with the orientation seen in the bulk structures of these materials and in previous TEM studies of comparable thickness films on KCl (001).<sup>1b,11</sup> The AFM images shown above, for C4-PTCDI on both the KCl and KBr surfaces suggest thin films that have achieved locally a coverage of 1–2 monolayers are strongly aggregated, with the perylene cores tilted away from a parallel orientation with respect to the surface plane. This imaged material must be responsible for the excimeric luminescence features, while residual flat-lying and isolated C4-PTCDI molecules and dye that exists at the borders of these aggregates (all unimaged to date) are responsible for the monomer-like luminescence signals.

Modeling protocols to describe the epitaxial relationships between organic monolayers and various single-crystal substrates have been developed that take into account the relationship between the unit-cell dimensions of the substrate and those of the unit cell of the organic monolayer.<sup>8</sup> Hillier and Ward showed that commensurate, versus coincident, versus incommensurate relationships could be discriminated by computation of the mismatch of the lattice vectors of the overlayer unit cell, at various azimuthal rotation angles, relative to those of the substrate.<sup>8a,c</sup> We have recently developed a computationally efficient version of this algorithm that takes into account certain lattice combinations not provided in their protocol.<sup>8b</sup> These protocols follow on the proposal by Hoshino et al. of “point-on-line” epitaxial relationships for the deposition of PTCDA on HOPG, which utilize many of the same principles to describe the epitaxial relationships between such large molecules and a single-crystal substrate.<sup>1f</sup>

Assumptions are made that the interactions with the substrate are weak enough to preclude reconstruction of that surface. At an azimuthal rotation where the overlayer unit cell can be described by vectors whose magnitudes are integral multiples of those of the substrate unit cell, within some predetermined error, a commensurate lattice is predicted. When two of the lattice vectors are integral multiples of the substrate

unit cell and two are not, a coincident lattice is found. (The two that are even multiples must be in the same column of the transformation matrix that describes the unit cell of the overlayer in terms of the surface unit cell of the substrate). Coincident overlayers are typically commensurate with the substrate typically every 2–7 unit cells, forming a superstructure of several overlayer molecules. This situation has been found to be quite common for the epitaxial growth of organic overlayers on various single-crystal surfaces, classically represented by the overlayers formed by PTCDA on HOPG, Au (111), MoS<sub>2</sub> (0001), and other substrates interacting weakly with this molecule.<sup>1d–g</sup> In these cases, monolayer unit cells are predicted and experimentally confirmed, which do not deviate by more than a few percent in each lattice dimension from a stable form of the bulk structure. When the interaction with the surface is sufficiently strong, a significant reorganization of the overlayer unit cell can occur (e.g., PTCDA on Cu (100)), to form a commensurate lattice with the surface that does deviate significantly from the bulk structure for a single layer.<sup>1c</sup>

Using both our modeling protocols and those of Hillier and Ward, coincident superstructures ( $b_1 = 1.223$  nm,  $b_2 = 1.918$  nm,  $R = 33.0^\circ$ ) are predicted to form for flat-lying PTCDA on the NaCl (001) surface. These dimensions are close to those of the  $\beta$ -polymorph of PTCDA found in earlier TEM studies, which exhibited an azimuthal rotation of  $31^\circ$  ( $b_1 = 1.245$  nm,  $b_2 = 1.930$  nm,  $\beta = 90^\circ$ ).<sup>1a</sup> It should be noted, however, that those studies also indicated PTCDA monolayer unit cells rotated with respect to the substrate lattice vectors by  $4^\circ$  and  $7^\circ$  (structures that maximized the overlap of the carbonyl oxygens with cation sites), structures that are not predicted by these modeling approaches, i.e., they involve introduction of excessive lattice distortions in the known PTCDA bulk structures.<sup>1a</sup> In addition, all of the modeling protocols discussed above indicate that a *commensurate* lattice structure should form for PTCDA on NaCl (001) ( $b_1 = 1.196$  nm,  $b_2 = 1.994$  nm,  $\beta = 90^\circ$ ;  $R = 45^\circ$ ),<sup>8b</sup> which was not observed in the earlier TEM studies.

On KCl and KBr coincident PTCDA lattice structures are predicted to form. KCl:  $b_1 = 1.219$  nm,  $b_2 = 1.954$  nm,  $R = 1.9^\circ$  and  $b_1 = 1.188$  nm,  $b_2 = 1.920$  nm,  $R = 23^\circ$ ; KBr:  $b_1 = 1.260$  nm,  $b_2 = 2.006$  nm,  $R = 23.3^\circ$ . The structures with the largest azimuthal rotations appear to agree reasonably closely with the structures and azimuthal rotations determined from the TEM studies of PTCDA/KCl (001).<sup>1a</sup> In our studies to date, the PTCDA deposits on KCl and KBr tend to exhibit a more plateletlike morphology when compared with the dendritic growth seen on NaCl.

For the C4-PTCDI system TEM studies by Yanagi and co-workers have suggested that an epitaxial layer can form on the KCl (001) surface, with the *ac* plane of this monoclinic structure parallel to the substrate (as in Figure 1b).<sup>1b</sup> Modeling studies indicate that several coincident lattice structures are obtainable for monolayers of this molecule, with either the *ac* plane down or the *ab* plane down, with less than 6% negative distortion in the dimensions of the *a* axis in the unit cell, less than 3% distortions in either the *b* or *c* axis dimensions, and less than  $1^\circ$  alteration in the internal

angles of the monoclinic unit cell. Within these constraints, coincident superstructures are predicted for C4-PTCDI with the *ac* plane down at azimuthal rotations of 45° (KCl (001) and KBr (001)) and  $\pm 9.8^\circ$  (NaCl (001)). It is interesting to note that an azimuthal rotation of  $\pm 9.8^\circ$  is close to the orientation observed for the macroscopic crystals seen in Figure 3a, where the interaction of the first monolayer with the NaCl surface appears to be relatively weak, and C4-PTCDI quickly establishes a different (bulklike) growth motif relative to that seen for KCl and KBr surfaces. For C4-PTCDI with the *ab* plane down, coincident superstructures are predicted at azimuthal rotations of 45° for all three substrates, along with a few other azimuthal rotation angles. In addition, flat-lying structures are possible for this molecule on the three substrates investigated, with the same constraints indicated for flat-lying PTCDA monolayers, provided that the butyl chains can tilt away from the surface, and/or lie flat, creating more distance between adjacent perylene cores.

For multilayer depositions of C4-PTCDI, the only orientation that would appear to favor layer-by-layer growth is the one in which the *ac* plane is parallel to the substrate. This orientation also achieves the highest molecular density of perylene dye on the surface, which has been shown to be a driving force in the formation of crystalline molecular materials.<sup>24</sup> Given the degree of coincidence for both the *ac* and *ab* planes of this perylene bisimide with these substrates, it is not surprising to see a significant contribution of disordered

material in the luminescence spectra of the first deposited layers, in contrast to PTCDA, since these spectroscopic properties are expected to arise at the intersection points between misaligned nanometer-scale crystallites. In our studies in progress, however, it is clear that more conformal thin films are achievable for this type of bisimide material, as opposed to the parent dianhydride. As the length and chemical functionality of the side chain is increased in comparable perylene bis(dicarboximide) dyes, different layered configurations can be achieved, and liquid-crystalline character may be observed for some substituents.<sup>25</sup> The extent to which these configurations cause differences in exciton diffusion lengths and exciton dissociation probabilities at a perylene/phthalocyanine interface is under investigation.

**Acknowledgment.** We gratefully acknowledge many helpful discussions with H. Yanagi (Kobe University) regarding the properties of C4-PTCDI thin films. This research was supported in part by grants from the National Science Foundation (Chemistry), by the Office of Naval Research (Center for Advanced Multifunctional Polymers and Molecular Materials), a joint NSF-DAAD travel grant (T.F.), and by the Materials Characterization Program, State of Arizona. D.S. was supported in part by a DFG Habilitandenstipendium (Schl 340(3-1)), and A.B. was supported by an NSF Graduate Fellowship.

CM970589+

(24) (a) Perlstein, J. *Chem. Mater.* **1994**, *6*, 319. (b) Perlstein, J. *J. Am. Chem. Soc.* **1994**, *114*, 1955. (c) Perlstein, J. *J. Am. Chem. Soc.* **1994**, *116*, 11420.

(25) (a) Parkinson, B. A., personal communication. (b) Gregg, B. A., personal communication.